IEEE Access
Multidisciplinary | Rapid Review | Open Access Journal

Received October 6, 2017, accepted November 5, 2017, date of publication November 21, 2017, date of current version March 12, 2018.

Digital Object Identifier 10.1109/ACCESS.2017.2773709

Topology-Aware Space-Time Network Coding in Cellular Networks

RODOLFO TORREA-DURAN[1], (Member, IEEE), MÁXIMO MORALES CÉSPEDES[2], (Member, IEEE), JORGE PLATA-CHAVES[1], (Member, IEEE), LUC VANDENDORPE[2], (Fellow, IEEE), AND MARC MOONEN[1], (Fellow, IEEE)

[1]Center for Dynamical Systems, Department of Electrical Engineering, Signal Processing and Data Analytics, STADIUS, KU Leuven, 3000 Leuven, Belgium
[2]Digital Communications Group, ICTEAM Institute, Université Catholique de Louvain, 1348 Louvain-la-Neuve, Belgium

Corresponding author: Rodolfo Torrea-Duran (rodolfo.torreaduran@esat.kuleuven.be)

ABSTRACT Space-time network coding (STNC) is a time-division multiple access (TDMA)-based scheme that combines network coding and space-time coding by allowing relay nodes to combine the information received from different source nodes during the transmission phase and to forward the combined signal to a destination node in the relaying phase. However, STNC schemes require all the relay nodes to overhear the signals transmitted from all the source nodes in the network. They also require a large number of time-slots to achieve full diversity in a multipoint-to-multipoint transmission. Both conditions are particularly challenging for large cellular networks where, assuming a downlink transmission, base stations (BSs) and users only overhear a subset of all the BSs. In this paper, we exploit basic knowledge of the network topology in order to reduce the number of time-slots by allowing simultaneous transmissions from those BSs that do not overhear each other. Our results show that these topology-aware schemes are able to increase the spectral efficiency per time-slot and bit error rate with unequal transmit power and channel conditions.

INDEX TERMS Space-time network coding, network topology, cellular networks.

I. INTRODUCTION

Cooperative communication has emerged as a promising solution to satisfy the ever-increasing demand in wireless connectivity. Cooperative protocols exploit the broadcast nature of the wireless channel by allowing relay nodes to retransmit the overheard information to the destination nodes. This is usually done in two phases. In the first phase, the source nodes broadcast the information, which is received by the destination nodes and the relays. In the second phase, the relays forward this information to the destination nodes, which combine it with the information received from the source nodes in the first phase.

The cooperation between spatially distributed nodes requires perfect timing and frequency synchronization of the received signals. This is in practice a challenging task, for instance timing synchronization requires signals from different source nodes to arrive simultaneously at a destination node. Imperfect frequency synchronization results from the difference in the local oscillator frequency of every node. These imperfections results in intersymbol interference, which can bring a severe degradation of the system performance [1], [2]. The most commonly-used technique to completely avoid the imperfect synchronization issue in multi-node systems is time-division multiple access (TDMA), in which each transmitting node (source or relay) takes a dedicated time-slot to transmit information.

Space-Time Network Coding (STNC) [3] has been proposed as a TDMA-based technique to achieve cooperation among the nodes in a network while avoiding the synchronization issues. It combines network coding and space-time coding by allowing signals coming from different source nodes during the transmission phase to be combined at the relays and then forwarded to destination nodes in dedicated time-slots during the relaying phase. Considering a system with L source nodes, M relays and 1 destination node, STNC is able to achieve full diversity order of $M + 1$ with $L + M$ time-slots. In [4] the outage probability of this multipoint-to-point (M2P) STNC scheme is analyzed using decode-and-forward relays, while in [5] its symbol error rate performance is analyzed over independent but not necessarily identically distributed Nakagami-m fading channels using amplify-and-forward relays. In [6] the authors incorporate to the previous scheme a transmit antenna selection and maximal-ratio combining in the source-destination and relay-destination links in order to maximize the instantaneous signal-to-noise ratio. Furthermore, in [7] a differential STNC

scheme has been proposed that can also achieve full diversity while overcoming the practical challenges of channel estimation at the receiver. A step towards increasing the capacity of STNC was taken in [8] and in [9], where the authors propose that each relay decodes the transmission not only from the source nodes but also from the previously-transmitting relays. Furthermore, the source nodes can also be used as relays (as assumed in this paper), avoiding in this way the deployment of additional relays, as proposed in clustering-based STNC [10] and optimal node selection-based STNC schemes [11].

M2P STNC can be translated into a point-to-multipoint (P2M) scheme by instead considering a single source node transmitting to multiple destination nodes. It can also be translated into a multipoint-to-multipoint (M2M) scheme by combining the previous schemes [3].

A main disadvantage of the previous schemes is that they require that all the M relays (or the L source nodes acting as relays) overhear the signals transmitted by the L source nodes in order to forward the overheard information to the destination nodes. In a cellular downlink transmission for instance, relays (or base stations acting as relays) and users typically overhear only a subset of all the base stations (BSs), i.e. the closest BSs, and treat the other transmissions as noise [12]. Therefore, relay retransmissions are only useful to the closest users. Furthermore, the previous schemes require dedicated time-slots for each transmission in order to achieve full diversity order. These conditions render these schemes impractical in particular for large networks.

In this paper we exploit basic knowledge of the network topology, i.e. the knowledge of the different subsets of BSs that can be overheard by other BSs and users. In this way, we are able to reduce the number of time-slots and hence make our schemes practical for large networks. This can be done in two ways: firstly by allowing simultaneous transmissions from the BSs that do not overhear each other, which can be done both during the transmission and during the relaying phase. Secondly, by allowing all the BSs to transmit the overheard information in a single time-slot during the relaying phase instead of using dedicated time-slots. This last scheme comes with an imperfect synchronization during the single time-slot of the relaying phase. However, recent advances in delay-tolerant codes [13] or joint frequency and timing synchronization [2] show that this issue can be mitigated.

We analyze in this paper both proposed schemes in terms of spectral efficiency and bit error rate (BER). Our analytical and numerical results show that the topology-aware schemes are able to reduce drastically the number of time-slots and increase the spectral efficiency compared to traditional STNC, with a marginal decrease in the spatial diversity. Furthermore, we are able to compute closed-form expressions for the spectral efficiency and BER for any number of nodes, which allows us to analyze and predict the achievable gains for any network size and to compare it with other TDMA-based schemes.

This paper is organized as follows. In Section II the system model is presented. Section III provides a brief overview of the baseline schemes used for benchmarking. In Section IV the proposed topology-aware schemes are presented. Section V provides some simulation results where the performance of the proposed schemes is compared with the baseline schemes. Finally, Section VI provides concluding remarks.

II. SYSTEM MODEL

We consider a downlink cellular network with L single-antenna BSs, each of which has data intended for a specific user. To avoid the deployment of relays it is assumed that each BS can also act as a relay. It is assumed that the BSs and the users are half-duplex, i.e., they cannot transmit and receive simultaneously. The available network topology knowledge is limited to the knowledge of the different subsets of BSs that can be overheard by other BSs and users. We assume that there is no backhaul link between BSs (or that it is only used for transmitting control information), which excludes the use of transmission schemes that require data sharing among the BSs. Since we consider single-antenna BSs, notice that this condition excludes the use of space-time block codes, e.g., Alamouti codes. It is assumed that the intracell interference is avoided through orthogonal multiple access techniques, e.g., orthogonal frequency division multiple access (OFDMA), so that only the intercell interference is considered. In this context, the user connected to the l-th BS, which is referred to as Ul, is only subject to intercell interference from other BSs. Specifically, we consider a topological scheme where Ul receives all the signals from the cluster $\mathcal{C}_l$ composed by BSl and the neighboring $2K$ BSs. BSl can also overhear the transmission from the other BSs inside cluster $\mathcal{C}_l$. The transmissions from the BSs outside the cluster is then treated as noise.

For the sake of simplicity, we focus on the widely-used linear Wyner model [14] to formulate the considered system, as shown in Fig. 1. We assume a symmetric scenario where the BSs of $\mathcal{C}_l$ correspond to the K BSs on the left (numbered BS$(l-K), \ldots,$ BS$(l-1)$) and the K BSs on the right (numbered BS$(l+1), \ldots,$ BS$(l+K)$) of BSl. We use shorthand notation with BS numbers to define clusters, e.g. $\mathcal{C}_l = \{l-K, \ldots, l-1, l, l+1, \ldots, l+K\}$. The BSs of cluster $\mathcal{C}_l$ that transmit in time-slot (TS) t are comprised in $\mathcal{C}_l^{(t)}$. Thus, assuming BS$l \in \mathcal{C}_l^{(t)}$, the signal received by Ul in TSt in the transmission phase can be written as

$$y_l^{(t)} = \sqrt{P_l} h_{l,l} s_l + \sum_{k \in \mathcal{C}_l^{(t)} \setminus l} i_{k,l}^{(t)} + n_l^{(t)}, \tag{1}$$

where $h_{k,l}$ is the channel between BSk and user Ul, which follows a Rayleigh distribution with zero mean and unit variance. Furthermore, P_l is the transmit power of BSl, s_l is the symbol transmitted by BSl intended for Ul, and $n_l^{(t)}$ is the additive white Gaussian noise (AWGN) with zero mean and variance σ_n^2, which is assumed to be equal for

TABLE 1. TDMA transmission strategy.

Time-slot	...	BS$(l-3)$	BS$(l-2)$	BS$(l-1)$	BSl	BS$(l+1)$	BS$(l+2)$	BS$(l+3)$	...
TS1	...	s_{l-3}		s_{l-1}		s_{l+1}		s_{l+3}	...
TS2	...		s_{l-2}		s_l		s_{l+2}		...

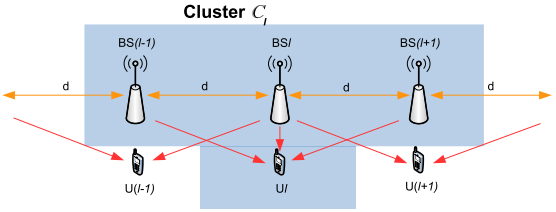

FIGURE 1. Wyner model for a cellular network. The cluster considers the $2K$ closest BSs, i.e. $\mathcal{C}_l = \text{BS}\{l-1, l, l+1\}$ for $K = 1$, with a distance d between BSs.

all the users. The parameter $i_{k,l}^{(t)}$ denotes the interference received by Ul from BSk in TSt. Therefore, $\sum_{k\in\mathcal{C}_l^{(t)}\setminus l} i_{k,l}^{(t)}$ corresponds to the intercell interference within cluster $\mathcal{C}_l$. We also define $\gamma_{k,l} = \sqrt{P_k}h_{k,l}$, $\xi_{m,n} = \sqrt{P_m}g_{m,n}$, where $g_{m,n}$ is the channel between BSm and BSn, and $\sigma_{\text{s}}^2 = \mathbb{E}\{|s_l|^2\}$ $\forall l$. Finally, we assume that the channel coherence time is larger than the transmission round of each scheme, i.e. that the channel gains do not change within one transmission round.

III. BASELINE SCHEMES

This section presents the baseline schemes that will be used to benchmark the performance of the proposed topology-aware schemes.

A. SIMULTANEOUS TRANSMISSIONS SCHEME (INTF)

The simplest baseline scheme consists in all the BSs transmitting simultaneously regardless of the interference that they cause to the users. This means that the transmission phase has one time-slot ($t = 1$) and that there is no relaying phase. We refer to this scheme as INTF. The signal received by Ul in TSt ($t = 1$) is given by (1) with $\mathcal{C}_l^{(t)} = \mathcal{C}_l$.

Since each BSl transmits to its corresponding user Ul in every time-slot, the spectral efficiency per time-slot for Ul can be directly computed as

$$S_l^{\text{INTF}} = \mathbb{E}\left\{\log_2\left(1 + \frac{|\gamma_{l,l}|^2\sigma_{\text{s}}^2}{\sigma_{\text{n}}^2 + \sum\limits_{\substack{k=l-K\\k\neq l}}^{l+K}|\gamma_{k,l}|^2\sigma_{\text{s}}^2}\right)\right\}. \quad (2)$$

Notice that the use of every available time-slot by every BS typically leads to a considerable degradation in equivalent signal-to-interference-and-noise ratio (SINR) since the received signal is polluted by the interference from the surrounding BSs.

Using a minimum mean square error (MMSE) receiver with BPSK modulation over a Rayleigh fading channel (assumptions holding throughout this paper), the BER can be computed in terms of the Q function as

$$\text{BER}_l^{\text{INTF}} = \mathbb{E}\left\{Q\left(\sqrt{2\gamma_{\text{INTF}}}\right)\right\}, \quad (3)$$

where $\gamma_{\text{INTF}} = |\gamma_{l,l}|^2\sigma_{\text{s}}^2 / \left(\sigma_{\text{n}}^2 + \sum_{\substack{k=l-K\\k\neq l}}^{l+K}|\gamma_{k,l}|^2\sigma_{\text{s}}^2\right)$.

B. ORTHOGONAL TRANSMISSIONS SCHEME (TDMA)

For an orthogonal scheme such as TDMA, the communication is done in turns. Since two BSs separated by $K + 1$ BSs do not overhear each other, they can transmit simultaneously. For instance, in TS1, BS$(l - K)$ and BS$(l + 1)$ can transmit s_{l-K}, and s_{l+1} simultaneously to their corresponding user, while the other BSs of $\mathcal{C}_l$ are inactive. Then in TS2, BS$(l - K + 1)$ and BS$(l + 2)$ can transmit s_{l-K+1}, and s_{l+2} simultaneously to their corresponding user, while the other BSs of $\mathcal{C}_l$ are inactive. The process continues until in TS$(K + 1)$ BSl transmits s_l to Ul. This allows a similar strategy in the rest of the network and hence the interference from neighboring BSs can be completely avoided. The transmission strategy of this topology-aware TDMA for a cluster of 3 BSs ($K = 1$) is summarized in Table 1 (the shaded part corresponds to $\mathcal{C}_l$).

For this TDMA scheme, the signal received by user Ul from BSl in TSt, i.e. in the time-slot in which the user is served, can be written as

$$y_l^{(t)} = \sqrt{P_l}h_{l,l}s_l + n_l^{(t)}. \quad (4)$$

Since $K + 1$ time-slots are required to complete the transmission to all the users, the spectral efficiency per time-slot of TDMA for Ul can be directly computed as

$$S_l^{\text{TDMA}} = \frac{1}{K+1}\mathbb{E}\left\{\log_2\left(1 + \frac{|\gamma_{l,l}|^2\sigma_{\text{s}}^2}{\sigma_{\text{n}}^2}\right)\right\}. \quad (5)$$

Notice the pre-log factor of $\frac{1}{K+1}$, which can be interpreted as the multiplexing gain.

The BER of Ul can be computed as [15]

$$\begin{aligned}\text{BER}_l^{\text{TDMA}} &= \mathbb{E}\left\{Q\left(\sqrt{\frac{2|\gamma_{l,l}|^2\sigma_{\text{s}}^2}{\sigma_{\text{n}}^2}}\right)\right\}\\ &= \frac{1}{\pi}\int_0^{\pi/2}\left(\frac{1}{1+\frac{\bar{\gamma_{l,l}}}{\sin^2\phi}}\right)d\phi \approx \frac{1}{\bar{\gamma_{l,l}}}, \end{aligned} \quad (6)$$

where $\bar{\gamma_{k,l}} = \mathbb{E}\{|\gamma_{k,l}|^2\}\frac{\sigma_{\text{s}}^2}{\sigma_{\text{n}}^2} = \frac{P_k\mathbb{E}\{|h_{k,l}|^2\}\sigma_{\text{s}}^2}{\sigma_{\text{n}}^2}$ and the approximation holds in the high SNR regime [16]. From the last approximation of equation (6), it can be seen that the BER is independent of K and hence no diversity gain is achieved.

TABLE 2. mSTNC transmission strategy ($K = 1$).

Time-slot	...	BS$(l-3)$	BS$(l-2)$	BS$(l-1)$	BSl	BS$(l+1)$	BS$(l+2)$	BS$(l+3)$	...
TS1	...			s_{l-1}			s_{l+2}		...
TS2	...	s_{l-3}			s_l			s_{l+3}	...
TS3	...		s_{l-2}			s_{l+1}			...
TS4	...			s_l			s_{l+3}		...
TS5	...	s_{l-2}			s_{l+1}			s_{l+4}	...
TS6	...		s_{l-1}			s_{l+2}			...
TS7	...			s_{l-2}			s_{l+1}		...
TS8	...	s_{l-4}			s_{l-1}			s_{l+2}	...
TS9	...		s_{l-3}			s_l			...

C. MODIFIED STNC (MSTNC)

In order to achieve full diversity in a scenario where BSs and users overhear the BSs inside their cluster, we require the use of dedicated time-slots per transmission. Hence, here we redefine the M2M transmission scheme using STNC presented in [3] for this scenario. We refer to this scheme as mSTNC, which can be explained as follows.

In a first (transmission) phase each BS of the considered cluster $\mathcal{C}_l$ transmits the symbol intended for its corresponding user in a dedicated time-slot while all the other BSs in $\mathcal{C}_l$ (as well as in the cluster of the transmitting BSs) remain silent. In a second (relaying) phase, each BS of cluster $\mathcal{C}_l$ transmits one of the symbols overheard in the first phase in a dedicated time-slot. In a third (relaying) phase, each BS of cluster $\mathcal{C}_l$ transmits another of the symbols overheard in the first phase in a dedicated time-slot. This process continues until in phase $2K+1$ each BS of cluster $\mathcal{C}_l$ transmits the last of the symbols overheard in the first phase in a dedicated time-slot. Hence this scheme requires $(2K+1)^2$ time-slots for one transmission round.

The transmission strategy of mSTNC for $K = 1$ is summarized in Table 2 (the shaded part corresponds to $\mathcal{C}_l$). Focusing on the l-th user, the symbol s_l is received in three time-slots (TS2, TS4, and TS9) corresponding to the transmission from BSs $\{l, l-1, l+1\}$. Specifically, the received signal can then be expressed as

$$\begin{aligned} y_l^{(2)} &= \sqrt{P_l} h_{l,l} s_l + n_l^{(2)} \\ y_l^{(4)} &= \sqrt{P_{l-1}} h_{l-1,l} z_{l,l-1}^{(2)} + n_l^{(4)} \\ y_l^{(9)} &= \sqrt{P_{l+1}} h_{l+1,l} z_{l,l+1}^{(2)} + n_l^{(9)} \end{aligned} \tag{7}$$

where the relayed symbol $z_{m,n}^{(t)}$ is defined as

$$z_{m,n}^{(t)} = s_m + \frac{n_{\mathrm{BS}n}^{(t)}}{\sqrt{P_m} g_{m,n}}, \tag{8}$$

where $n_{\mathrm{BS}n}^{(t)}$ is the AWGN noise received by BSn in TSt with zero mean and variance also assumed to be equal to σ_{n}^2. Notice that the interference from the BSs inside cluster $\mathcal{C}_l$ is completely avoided.

The spectral efficiency per time-slot of mSTNC for Ul (calculated as described in Section IV) can be directly computed as

$$S_l^{\mathrm{mSTNC}} = \frac{1}{(2K+1)^2} \mathbb{E}\left\{\log_2\left(1+\gamma_{\mathrm{mSTNC}}\right)\right\}, \tag{9}$$

where

$$\gamma_{\mathrm{mSTNC}} = \frac{|\gamma_{l,l}|^2 \sigma_{\mathrm{s}}^2}{\sigma_{\mathrm{n}}^2} + \sum_{\substack{k=l-K \\ k\neq l}}^{l+K} \frac{|\gamma_{k,l}|^2 \sigma_{\mathrm{s}}^2}{\frac{|\gamma_{k,l}|^2 \sigma_{\mathrm{n}}^2}{|\xi_{l,k}|^2} + \sigma_{\mathrm{n}}^2} \tag{10}$$

Notice that mSTNC ensures that each user receives its symbol from the $2K+1$ BSs of the cluster in dedicated time-slots.

The BER of Ul can be computed as

$$\mathrm{BER}_l^{\mathrm{mSTNC}} = \mathbb{E}\left\{Q\left(\sqrt{2\gamma_{\mathrm{mSTNC}}}\right)\right\}. \tag{11}$$

Since γ_{mSTNC} is not affected by any interference from other BSs within cluster $\mathcal{C}_l$, mSTNC can achieve full diversity gain of $2K+1$.

IV. TOPOLOGY-AWARE STNC (TAS)

While INTF provides full multiplexing gain, it comes with a large interference from the neighboring BSs. On the other hand, mSTNC provides full diversity gain with a large number of time-slots. Exploiting the topology of the network can provide a trade-off between diversity and multiplexing gain. We propose two schemes to achieve this. The first scheme consists in allowing simultaneous transmissions from the BSs that do not overhear each other both during the transmission phase and during the relaying phase. We refer to it as TAS1. A second scheme consists in allowing simultaneous transmissions as in TAS1 during the transmission phase, while during the relaying phase all the BSs transmit the overheard information in a single time-slot. We refer to it as TAS2. These schemes are described in the next two sections.

A. SIMPLE CASE WITH $K = 1$

In this scenario each user receives the transmissions from the closest 3 BSs. Similarly, each BS overhears the transmissions from the closest 2 BSs (one to the right and one to the left). Therefore, all the even-numbered BSs will not cause interference to any particular user when transmitting simultaneously, and neither will the odd-numbered BSs when transmitting simultaneously. Based on this, the proposed schemes work as follows.

In TS1, BS($l-1$) and BS($l+1$) transmit simultaneously the symbol intended for their corresponding user, i.e. s_{l-1} and s_{l+1}, respectively, as shown in Fig. 2(a). Hence, U($l-1$) and U($l+1$) receive their desired symbol without interference from other BSs. BSl and Ul also overhear a combination of symbols s_{l-1} and s_{l+1}. The transmissions from each base station are assumed to be synchronized such that they are received simultaneously. In TS2 BSl transmits s_l avoiding the interference from the BSs in cluster $\mathcal{C}_l$ as shown in Fig. 2(b). This means that Ul receives s_l without interference from other BSs. Due to the overhearing capabilities of the network, BS($l-1$) and BS($l+1$) (and also U($l-1$) and U($l+1$)) receive a combination of symbols including s_l. The transmission phase thus corresponds to TDMA (Table 1). The relaying phase is different between TAS1 and TAS2. For TAS1, in TS3 BS($l-1$) and BS($l+1$) transmit simultaneously the combination of overheard symbols from TS2 as shown in Fig. 2(c). Finally in TS4, BSl transmits the combination of the overheard symbols s_{l-1} and s_{l+1} from TS1 as shown in Fig. 2(d). For TAS2, in TS3 each BS transmits simultaneously the combination of overheard symbols from TS1 or TS2 as shown in Fig. 2(e). As a result, in both schemes Ul receives its desired symbol s_l from all the BSs in cluster $\mathcal{C}_l$ in one transmission round. The transmission strategy of the proposed schemes for $K = 1$ is summarized in Table 3 for TAS1 and Table 4 for TAS2. Note that the BSs outside the cluster have a similar transmission scheme.

For TAS1, the received signals for Ul can be expressed as

$$\begin{aligned} y_l^{(1)} &= \sqrt{P_{l-1}}h_{l-1,l}s_{l-1} + \sqrt{P_{l+1}}h_{l+1,l}s_{l+1} + n_l^{(1)} \\ y_l^{(2)} &= \sqrt{P_l}h_{l,l}s_l + n_l^{(2)} \\ y_l^{(3)} &= \sqrt{P_{l-1}}h_{l-1,l}\psi_{l-1} + \sqrt{P_{l+1}}h_{l+1,l}\psi_{l+1} + n_l^{(3)} \\ y_l^{(4)} &= \sqrt{P_l}h_{l,l}\psi_l + n_l^{(4)}, \end{aligned} \tag{12}$$

where the relayed symbols are normalized by the total received power to avoid exceeding the maximum transmit power:

$$\psi_k = \frac{\sqrt{P_{k-1}}g_{k-1,k}s_{k-1} + \sqrt{P_{k+1}}g_{k+1,k}s_{k+1} + n_{\mathrm{BS}k}^{(\tau)}}{\tilde{P}_{k-1,k}} \tag{13}$$

where τ is the time-slot in which BSk receives the transmission from BS($k-1$) and BS($k+1$) and $\tilde{P}_{m,k} = P_m|g_{m,k}|^2 + P_{m+K+1}|g_{m+K+1,k}|^2 + \frac{\sigma_{\mathrm{n}}^2}{\sigma_{\mathrm{s}}^2}$, corresponding to the power received by BSk from BSm and from BS($m+K+1$). For $K = 1$, $m = k-1$ and $m+K+1 = k+1$. Notice that the normalization is such that the transmission power in the relaying phase is equal to the transmission power in the transmission phase.

For TAS2, the received signals for Ul can be expressed as

$$\begin{aligned} y_l^{(1)} &= \sqrt{P_{l-1}}h_{l-1,l}s_{l-1} + \sqrt{P_{l+1}}h_{l+1,l}s_{l+1} + n_l^{(1)} \\ y_l^{(2)} &= \sqrt{P_l}h_{l,l}s_l + n_l^{(2)} \\ y_l^{(3)} &= \sqrt{P_l}h_{l,l}\psi_l^{(1)} + \sum_{\substack{k=l-1 \\ k\neq l}}^{l+1} \sqrt{P_k}h_{k,l}\psi_k^{(2)} + n_l^{(3)}. \end{aligned} \tag{14}$$

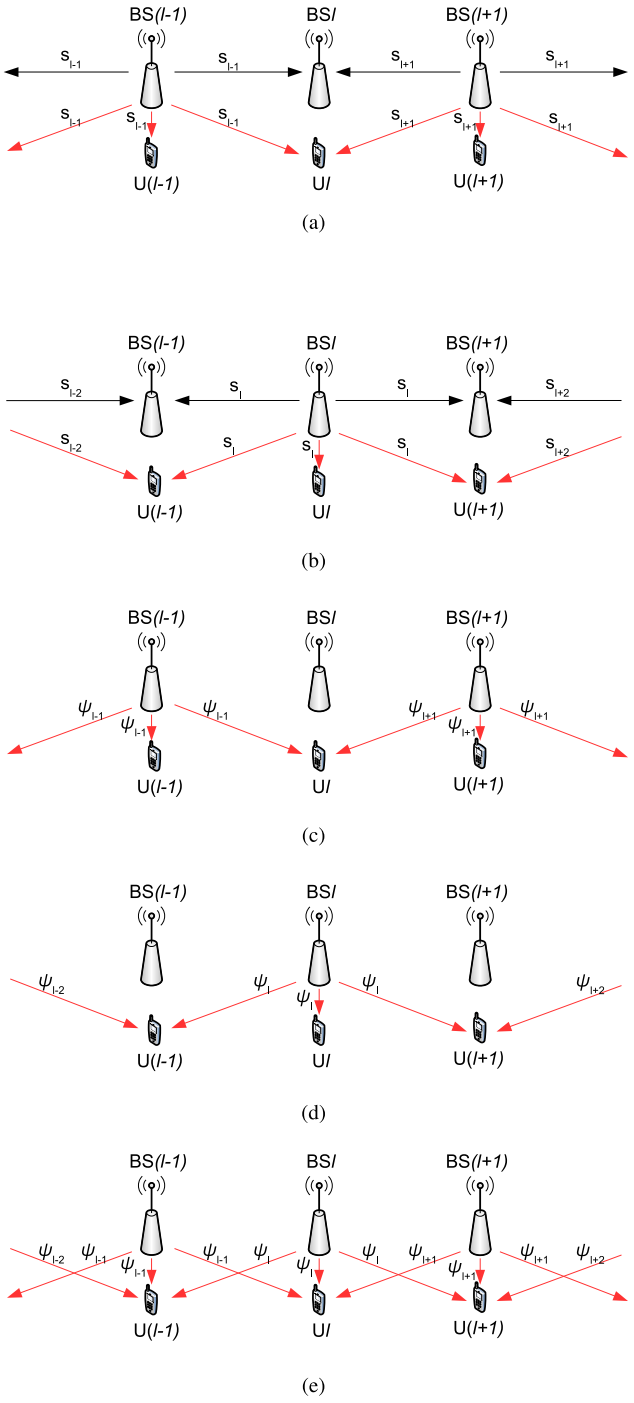

FIGURE 2. Transmission strategy of the proposed TAS1 and TAS2 for $K = 1$. (a) Transmission phase TAS1 and TAS2. BS($l-1$) $\rightarrow s_{l-1}$ and BS($l+1$) $\rightarrow s_{l+1}$. (b) Transmission phase TAS1 and TAS2. BSl $\rightarrow s_l$. (c) Relaying phase TAS1. BS($l-1$) $\rightarrow s_{l-2} + s_l$ and BS($l+1$) $\rightarrow s_l + s_{l+2}$. (d) Relaying phase TAS1. BSl $\rightarrow s_{l-1} + s_{l+1}$. (e) Relaying phase TAS2. BS($l-1$) $\rightarrow s_{l-2} + s_l$, BS$l$ $\rightarrow s_{l-1} + s_{l+1}$, and BS($l+1$) $\rightarrow s_l + s_{l+2}$.

Notice that the desired symbol s_l for Ul is received from three signal paths. Specifically, from its corresponding BSl in a dedicated time-slot during the transmission phase and from BS($l-1$) and BS($l+1$) during the relaying phase.

TABLE 3. TAS1 transmission strategy ($K = 1$).

Time-slot	...	BS$(l-3)$	BS$(l-2)$	BS$(l-1)$	BSl	BS$(l+1)$	BS$(l+2)$	BS$(l+3)$	...
TS1	...	s_{l-3}		s_{l-1}		s_{l+1}		s_{l+3}	...
TS2	...		s_{l-2}		s_l		s_{l+2}		...
TS3	...	$s_{l-4}+$ s_{l-2}		$s_{l-2}+$ s_l		s_l+ s_{l+2}		$s_{l+2}+$ s_{l+4}	...
TS4	...		$s_{l-3}+$ s_{l-1}		$s_{l-1}+$ s_{l+1}		$s_{l+1}+$ s_{l+3}		...

TABLE 4. TAS2 transmission strategy ($K = 1$).

Time-slot	...	BS$(l-3)$	BS$(l-2)$	BS$(l-1)$	BSl	BS$(l+1)$	BS$(l+2)$	BS$(l+3)$	...
TS1	...	s_{l-3}		s_{l-1}		s_{l+1}		s_{l+3}	...
TS2	...		s_{l-2}		s_l		s_{l+2}		...
TS3	...	$s_{l-4}+$ s_{l-2}	$s_{l-3}+$ s_{l-1}	$s_{l-2}+$ s_l	$s_{l-1}+$ s_{l+1}	s_l+ s_{l+2}	$s_{l+1}+$ s_{l+3}	$s_{l+2}+$ s_{l+4}	...

To represent the normalized channels effectively used to relay the overheard symbols during the relaying phase let us define

$$\eta_{m,l}^{v,w} = \frac{\gamma_{m,l}\xi_{v,m}}{\tilde{P}_{w,m}}, \tag{15}$$

corresponding to the relaying of s_v from BSm to Ul, normalized by the power received by BSm resulting from the transmission from BSw and from BS$(w+K+1)$ (one of which is also BSv).

Equation (12) can then be expressed in a matrix form as (16), as shown at the bottom of this page, and equation (14) as (17), as shown at the bottom of this page.

In the next section, we derive the general expressions of the received signal for a general $K \geq 1$ and then compute the achieved spectral efficiency.

B. GENERAL CASE WITH $K \geq 1$

In TS1 of the transmission phase a first pair of BSs within cluster $\mathcal{C}_l$ *that do not overhear each other* (nor do they overhear the transmitting BSs in other clusters), i.e. BS$(l-K)$ and BS$(l+1)$, transmit simultaneously the symbol intended for their corresponding user, i.e. s_{l-K} and s_{l+1}, respectively. In TS2 the next pair of BSs, i.e. BS$(l-K+1)$ and BS$(l+2)$, transmit s_{l-K+1} and s_{l+2}, respectively. This continues until finally, in TS$(K+1)$ the middle BS of cluster $\mathcal{C}_l$, i.e. BSl, transmits s_l. Meanwhile, the BSs outside cluster $\mathcal{C}_l$ can use a similar transmission strategy. The transmission phase thus corresponds to TDMA. Once the transmission phase ($K+1$ time-slots) concludes, each BS has overheard the combination of the symbols from its $2K$ neighboring BSs. For TAS1, in the relaying phase ($K+1$ time-slots) the same pairs of BSs transmit the combination of overheard symbols in dedicated time-slots. For TAS2 in the relaying phase (1 time-slot), all the BSs transmit simultaneously the combination of overheard symbols.

For TAS1, the received signals for Ul can be expressed as

$$\begin{aligned}
y_l^{(1)} &= \sqrt{P_{l-K}}h_{l-K,l}s_{l-K} + \sqrt{P_{l+1}}h_{l+1,l}s_{l+1} + n_l^{(1)}\\
y_l^{(2)} &= \sqrt{P_{l-K+1}}h_{l-K+1,l}s_{l-K+1} + \sqrt{P_{l+2}}h_{l+2,l}s_{l+2} + n_l^{(2)}\\
&\vdots\\
y_l^{(K+1)} &= \sqrt{P_l}h_{l,l}s_l + n_l^{(K+1)}\\
y_l^{(K+2)} &= \sqrt{P_{l-K}}h_{l-K,l}\Psi_{l-K} + \sqrt{P_{l+1}}h_{l+1,l}\Psi_{l+1} + n_l^{(K+2)}\\
y_l^{(K+3)} &= \sqrt{P_{l-K+1}}h_{l-K+1,l}\Psi_{l-K+1} + \sqrt{P_{l+2}}h_{l+2,l}\Psi_{l+2}\\
&\quad + n_l^{(K+3)}\\
&\vdots\\
y_l^{(2K+2)} &= \sqrt{P_l}h_{l,l}\Psi_l + n_l^{(2K+2)},
\end{aligned} \tag{18}$$

$$\mathbf{y}_l = \underbrace{\begin{bmatrix} 0 & \gamma_{l-1,l} & 0 & \gamma_{l+1,l} & 0\\ 0 & 0 & \gamma_{l,l} & 0 & 0\\ \eta_{l-1,l}^{l-2,l-2} & 0 & \eta_{l-1,l}^{l,l-2}+\eta_{l+1,l}^{l,l} & 0 & \eta_{l+1,l}^{l+2,l}\\ 0 & \eta_{l,l}^{l-1,l-1} & 0 & \eta_{l,l}^{l+1,l-1} & 0 \end{bmatrix}}_{\mathbf{C}} \begin{bmatrix} s_{l-2}\\ s_{l-1}\\ s_l\\ s_{l+1}\\ s_{l+2} \end{bmatrix} + \begin{bmatrix} n_l^{(1)}\\ n_l^{(2)}\\ n_l^{(3)} + \frac{\gamma_{l-1,l}n_{\mathrm{BS}(l-1)}^{(2)}}{\tilde{P}_{l-2,l-1}} + \frac{\gamma_{l+1,l}n_{\mathrm{BS}(l+1)}^{(2)}}{\tilde{P}_{l,l+1}}\\ n_l^{(4)} + \frac{\gamma_{l,l}n_{\mathrm{BS}l}^{(1)}}{\tilde{P}_{l-1,l}} \end{bmatrix} \tag{16}$$

$$\mathbf{y}_l = \underbrace{\begin{bmatrix} 0 & \gamma_{l-1,l} & 0 & \gamma_{l+1,l} & 0\\ 0 & 0 & \gamma_{l,l} & 0 & 0\\ \eta_{l-1,l}^{l-2,l-2} & \eta_{l,l}^{l-1,l-1} & \eta_{l-1,l}^{l,l-2}+\eta_{l+1,l}^{l,l} & \eta_{l,l}^{l+1,l-1} & \eta_{l+1,l}^{l+2,l} \end{bmatrix}}_{\mathbf{B}} \begin{bmatrix} s_{l-2}\\ s_{l-1}\\ s_l\\ s_{l+1}\\ s_{l+2} \end{bmatrix} + \begin{bmatrix} n_l^{(1)}\\ n_l^{(2)}\\ n_l^{(3)} + \frac{\gamma_{l,l}n_{\mathrm{BS}l}^{(1)}}{\tilde{P}_{l-1,l}} + \frac{\gamma_{l-1,l}n_{\mathrm{BS}(l-1)}^{(2)}}{\tilde{P}_{l-2,l-1}} + \frac{\gamma_{l+1,l}n_{\mathrm{BS}(l+1)}^{(2)}}{\tilde{P}_{l,l+1}} \end{bmatrix} \tag{17}$$

where

$$\Psi_k = \frac{1}{K}\sum_{m=1}^{K} \frac{\begin{pmatrix}\sqrt{P_{k-K+m-1}}g_{k-K+m-1,k}s_{k-K+m-1}+\\ \sqrt{P_{k+m}}g_{k+m,k}s_{k+m}+n_{\mathrm{BS}k}^{(\tau)}\end{pmatrix}}{\tilde{P}_{k-K+m-1,k}}. \quad (19)$$

Note that τ depends on m and k as it is is the time-slot in which BSk receives the transmissions from BS$(k-K+m-1)$ and BS$(k+m)$. Also note that each of the K terms of (19) is normalized independently, which requires a $1/K$ factor to have the same transmission power in the relaying phase and the transmission phase. The normalization is done independently for each term so that large differences in transmission power and/or average channel gains only affect the symbols relayed in a given time-slot.

For TAS2, the received signals for Ul can be expressed as

$$\begin{aligned} y_l^{(1)} &= \sqrt{P_{l-K}}h_{l-K,l}s_{l-K} + \sqrt{P_{l+1}}h_{l+1,l}s_{l+1} + n_l^{(1)} \\ y_l^{(2)} &= \sqrt{P_{l-K+1}}h_{l-K+1,l}s_{l-K+1} + \sqrt{P_{l+2}}h_{l+2,l}s_{l+2} \\ &\quad + n_l^{(2)} \\ &\vdots \\ y_l^{(K+1)} &= \sqrt{P_l}h_{l,l}s_l + n_l^{(K+1)} \\ y_l^{(K+2)} &= \sqrt{P_l}h_{l,l}\Psi_l + \sum_{\substack{m=l-K \\ m\neq l}}^{l+K} \sqrt{P_m}h_{m,l}\Psi_m + n_l^{(K+2)} \end{aligned} \quad (20)$$

Following this scheme, the signal received by user Ul, $\mathbf{y}_l \in \mathbb{C}^{2(K+1)\times 1}$ for TAS1 and $\mathbf{y}_l \in \mathbb{C}^{(K+2)\times 1}$ for TAS2, can be written as equation (21), as shown at the bottom of this page, where diag($\mathbf{a}$) denotes the diagonal matrix with the vector $\mathbf{a}$ as the main diagonal, $\mathbf{s}_{\text{cluster}} = \text{col}\{s_{l'}\}_{l'=l-K}^{l+K}$ are the symbols intended for the users within cluster $\mathcal{C}_l$ and $\mathbf{s}_{\text{left}} = \text{col}\{s_{l'}\}_{l'=l-2K}^{l-K-1}$ and $\mathbf{s}_{\text{right}} = \text{col}\{s_{l'}\}_{l'=l+K+1}^{l+2K}$ are the symbols intended for the users outside the cluster to the left- and right-hand side, respectively. The first two rows of matrix $\mathbf{A}$ in equation (21), as shown at the bottom of this page, correspond to the transmission phase, which is equal for TAS1 and TAS2. However, the last row corresponds to the relaying phase, which is different for TAS1 and TAS2.

Recall that TAS1 uses a relaying phase of equal duration as the transmission phase. Moreover, during the relaying phase the combination of overheard symbols is transmitted by each BS in dedicated time-slots. Referring to the last block row in matrix $\mathbf{A}$ of (21), this results in matrices (22) and (23),that contain the channel entries for the symbols $\mathbf{s}_{\text{cluster}}$ corresponding to $\mathcal{C}_l$: $\mathbf{H}_{\text{cluster}_1}^{\text{TAS1}}$ contains the channel entries for the symbols relayed from the BSs of $\mathcal{C}_l$ to the left of BSl (including BSl) and $\mathbf{H}_{\text{cluster}_2}^{\text{TAS1}}$ contains the channel entries for the symbols relayed from the BSs of $\mathcal{C}_l$ to the right of BSl. Similarly,

$$\begin{aligned} \mathbf{H}_{\text{left}}^{\text{TAS1}} &= \begin{bmatrix} \eta_{l-K,l}^{l-2K,l-2K} & \eta_{l-K,l}^{l-2K+1,l-2K+1} & \cdots & \eta_{l-K,l}^{l-K-1,l-K-1} \\ 0 & \eta_{l-K+1,l}^{l-2K+1,l-2K+1} & \cdots & \eta_{l-K+1,l}^{l-K-1,l-K-1} \\ \vdots & \vdots & \ddots & \vdots \\ 0 & 0 & \cdots & \eta_{l-1,l}^{l-K-1,l-K-1} \\ 0 & 0 & \cdots & 0 \end{bmatrix} \\ &\in \mathbb{C}^{K+1\times K} \end{aligned} \quad (24)$$

and

$$\begin{aligned} \mathbf{H}_{\text{right}}^{\text{TAS1}} &= \begin{bmatrix} \eta_{l+1,l}^{l+K+1,l} & 0 & \cdots & 0 \\ \eta_{l+2,l}^{l+K+1,l} & \eta_{l+2,l}^{l+K+2,l+1} & \cdots & 0 \\ \vdots & \vdots & \ddots & \vdots \\ \eta_{l+K,l}^{l+K+1,l} & \eta_{l+K,l}^{l+K+2,l+1} & \cdots & \eta_{l+K,l}^{l+2K,l+K-1} \\ 0 & 0 & \cdots & 0 \end{bmatrix} \\ &\in \mathbb{C}^{K+1\times K} \end{aligned} \quad (25)$$

contain the channel entries for the symbols $\mathbf{s}_{\text{left}}$ and $\mathbf{s}_{\text{right}}$, respectively. Note that BSl transmits without interference

$$\mathbf{y}_l = \underbrace{\begin{bmatrix} \mathbf{0}_{K,K} & \text{diag}\left(\{\gamma_{l',l}\}_{l'=l-K}^{l-1}\right) & \mathbf{0}_{K,1} & \text{diag}\left(\{\gamma_{l',l}\}_{l'=l+1}^{l+K}\right) & \mathbf{0}_{K,K} \\ \mathbf{0}_{1,K} & & \gamma_{l,l} & & \mathbf{0}_{1,K} \\ \mathbf{H}_{\text{left}}^{\text{TAS}n} & & \mathbf{H}_{\text{cluster}_1}^{\text{TAS}n} + \mathbf{H}_{\text{cluster}_2}^{\text{TAS}n} & & \mathbf{H}_{\text{right}}^{\text{TAS}n} \end{bmatrix}}_{\mathbf{A}} \begin{bmatrix} \mathbf{s}_{\text{left}} \\ \mathbf{s}_{\text{cluster}} \\ \mathbf{s}_{\text{right}} \end{bmatrix} + \mathbf{n}_l \quad (21)$$

$$\begin{aligned} \mathbf{H}_{\text{cluster}_1}^{\text{TAS1}} &= \begin{bmatrix} 0 & \eta_{l-K,l}^{l-K+1,l-2K} & \cdots & \eta_{l-K,l}^{l-1,l-2-K} & \eta_{l-K,l}^{l,l-1-K} & 0 & 0 & \cdots & 0 \\ \eta_{l-K+1,l}^{l-K,l-K} & 0 & \cdots & \eta_{l-K+1,l}^{l-1,l-2-K} & \eta_{l-K+1,l}^{l,l-1-K} & \eta_{l-K+1,l}^{l+1,l-K} & 0 & \cdots & 0 \\ \vdots & \vdots & \ddots & \vdots & \vdots & \vdots & \vdots & \ddots & \vdots \\ \eta_{l-1,l}^{l-K,l-K} & \eta_{l-1,l}^{l-K+1,l-K+1} & \cdots & 0 & \eta_{l-1,l}^{l,l-1-K} & \eta_{l-1,l}^{l+1,l-K} & \eta_{l-1,l}^{l+2,l+1-K} & \cdots & 0 \\ \eta_{l,l}^{l-K,l-K} & \eta_{l,l}^{l-K+1,l-K+1} & \cdots & \eta_{l,l}^{l-1,l-1} & 0 & \eta_{l,l}^{l+1,l-K} & \eta_{l,l}^{l+2,l+1-K} & \cdots & \eta_{l,l}^{l+K,l-1} \end{bmatrix} \\ &\in \mathbb{C}^{K+1\times 2K+1} \end{aligned} \quad (22)$$

$$\begin{aligned} \mathbf{H}_{\text{cluster}_2}^{\text{TAS1}} &= \begin{bmatrix} 0 & \eta_{l+1,l}^{l-K+1,l-K+1} & \cdots & \eta_{l+1,l}^{l-1,l-1} & \eta_{l+1,l}^{l,l} & 0 & \eta_{l+1,l}^{l+2,l+1-K} & \cdots & \eta_{l+1,l}^{l+K,l-1} \\ 0 & 0 & \cdots & \eta_{l+2,l}^{l-1,l-1} & \eta_{l+2,l}^{l,l} & \eta_{l+2,l}^{l+1,l+1} & 0 & \cdots & \eta_{l+2,l}^{l+K,l-1} \\ \vdots & \vdots & \ddots & \vdots & \vdots & \vdots & \vdots & \ddots & \vdots \\ 0 & 0 & \cdots & 0 & \eta_{l+K,l}^{l,l} & \eta_{l+K,l}^{l+1,l+1} & \eta_{l+K,l}^{l+2,l+2} & \cdots & 0 \\ 0 & 0 & \cdots & 0 & 0 & 0 & 0 & \cdots & 0 \end{bmatrix} \\ &\in \mathbb{C}^{K+1\times 2K+1} \end{aligned} \quad (23)$$

from the other BSs in cluster $\mathcal{C}_l$ in the last time-slot of both phases. Specifically in the relaying phase, this transmission includes all the symbols of $\mathcal{C}_l$ except s_l.

Since TAS2 uses a relaying phase consisting of a single time-slot where the combination of overheard symbols is transmitted by all the BSs simultaneously, then the channel matrices are a row vector formed by the *summation* of the rows of $\mathbf{H}^{\text{TAS1}}_{\text{cluster}_1}$, $\mathbf{H}^{\text{TAS1}}_{\text{cluster}_2}$, $\mathbf{H}^{\text{TAS1}}_{\text{left}}$, and $\mathbf{H}^{\text{TAS1}}_{\text{right}}$, i.e.

$$\mathbf{H}^{\text{TAS2}}_{\text{cluster}_1} = \left[\sum_{m=1}^{K+1}\mathbf{h}^{\text{TAS1},1}_{\text{cluster}_1}(m) \ \sum_{m=1}^{K+1}\mathbf{h}^{\text{TAS1},2}_{\text{cluster}_1}(m) \ \cdots \ \sum_{m=1}^{K+1}\mathbf{h}^{\text{TAS1},2K+1}_{\text{cluster}_1}(m)\right] \in \mathbb{C}^{1\times 2K+1} \tag{26}$$

$$\mathbf{H}^{\text{TAS2}}_{\text{cluster}_2} = \left[\sum_{m=1}^{K+1}\mathbf{h}^{\text{TAS1},1}_{\text{cluster}_2}(m) \ \sum_{m=1}^{K+1}\mathbf{h}^{\text{TAS1},2}_{\text{cluster}_2}(m) \ \cdots \ \sum_{m=1}^{K+1}\mathbf{h}^{\text{TAS1},2K+1}_{\text{cluster}_2}(m)\right] \in \mathbb{C}^{1\times 2K+1} \tag{27}$$

$$\mathbf{H}^{\text{TAS2}}_{\text{left}} = \left[\sum_{m=1}^{K+1}\mathbf{h}^{\text{TAS1},1}_{\text{left}}(m) \ \sum_{m=1}^{K+1}\mathbf{h}^{\text{TAS1},2}_{\text{left}}(m) \ \cdots \ \sum_{m=1}^{K+1}\mathbf{h}^{\text{TAS1},K}_{\text{left}}(m)\right] \in \mathbb{C}^{1\times K} \tag{28}$$

$$\mathbf{H}^{\text{TAS2}}_{\text{right}} = \left[\sum_{m=1}^{K+1}\mathbf{h}^{\text{TAS1},1}_{\text{right}}(m) \ \sum_{m=1}^{K+1}\mathbf{h}^{\text{TAS1},2}_{\text{right}}(m) \ \cdots \ \sum_{m=1}^{K+1}\mathbf{h}^{\text{TAS1},K}_{\text{right}}(m)\right] \in \mathbb{C}^{1\times K} \tag{29}$$

where $\mathbf{h}^{\text{TAS}n,k}_{\text{text}}(m)$ is the m-th element of the k-th column of matrix $\mathbf{H}^{\text{TAS}n}_{\text{text}}$. In this way, it can be seen that for $K = 1$ equation (21) reduces to (16) for TAS1 and to (17) for TAS2.

The noise vector $\mathbf{n}_l$ of equation (21) is defined for TAS1 as

$$\mathbf{n}_l = \left[n_l^{(1)} \ \cdots \ n_l^{(K+1)} \left(n_l^{(K+2)} + \frac{1}{K}\sum_{m=1}^{K}\frac{\gamma_{l-K,l}\,n^{(\tau)}_{\text{BS}(l-K)}}{\tilde{P}_{l-2K+m-1,l-K}} + \frac{1}{K}\sum_{m=1}^{K}\frac{\gamma_{l+1,l}\,n^{(\tau)}_{\text{BS}(l+1)}}{\tilde{P}_{l-K+m,l+1}}\right) \left(n_l^{(K+3)} + \frac{1}{K}\sum_{m=1}^{K}\frac{\gamma_{l-K+1,l}\,n^{(\tau)}_{\text{BS}(l-K+1)}}{\tilde{P}_{l-2K+m,l-K+1}} + \frac{1}{K}\sum_{m=1}^{K}\frac{\gamma_{l+2,l}\,n^{(\tau)}_{\text{BS}(l+2)}}{\tilde{P}_{l+1-K+m,l+2}}\right) \cdots \left(n_l^{(2K+2)} + \frac{1}{K}\sum_{m=1}^{K}\frac{\gamma_{l,l}\,n^{(\tau)}_{\text{BS}l}}{\tilde{P}_{l-K+m-1,l}}\right)\right]^T \in \mathbb{C}^{1\times 2K+2} \tag{30}$$

and for TAS2 as

$$\mathbf{n}_l = \left[n_l^{(1)} \ \cdots \ n_l^{(K+1)} \left(n_l^{(K+2)} + \frac{1}{K}\sum_{k=l-K}^{l+K}\gamma_{k,l}\sum_{m=1}^{K}\frac{n^{(\tau)}_{\text{BS}k}}{\tilde{P}_{k-K+m-1,k}}\right)\right]^T \in \mathbb{C}^{1\times K+2} \tag{31}$$

C. PERFORMANCE ANALYSIS

Formula (21) can also be written as

$$\mathbf{y}_l = \sum_{k=l-2K}^{l+2K}\mathbf{a}_k s_k + \mathbf{n}_l = \mathbf{a}_l s_l + \mathbf{w}_l, \tag{32}$$

where $\mathbf{a}_l$ is the column of matrix $\mathbf{A}$ in (21) corresponding to s_l and $\mathbf{w}_l$ is the vector of interference plus noise

$$\mathbf{w}_l = \sum_{\substack{k=l-2K\\k\neq l}}^{l+2K}\mathbf{a}_k s_k + \mathbf{n}_l. \tag{33}$$

Using the well-known expression for the entropy of a multivariate complex Gaussian distribution [17] the capacity of the system is computed as

$$\log_2\frac{|\mathbf{R}_{\mathbf{y}_l}|}{|\mathbf{R}_{\mathbf{w}_l}|} = \log_2\left(1+\mathbf{a}_l^H\mathbf{R}_{\mathbf{w}_l}^{-1}\mathbf{a}_l\sigma_{\text{s}}^2\right) = \log_2\left(1+\text{SNR}_l^{\text{TAS}n}\right), \tag{34}$$

where $\text{SNR}_l^{\text{TAS}n}$ is the signal-to-noise ratio (SNR) of Ul using TASn and $|x|$ is the determinant of x. The covariance matrix of the received signal $\mathbf{R}_{\mathbf{y}_l}$ is given as

$$\mathbf{R}_{\mathbf{y}_l} = \mathbf{a}_l\mathbf{a}_l^H\sigma_{\text{s}}^2 + \mathbf{R}_{\mathbf{w}_l} \tag{35}$$

and the covariance matrix of the interference plus noise $\mathbf{R}_{\mathbf{w}_l}$ is given as

$$\mathbf{R}_{w_l} = \mathbb{E}\left\{\left(\sum_{\substack{k=l-2K\\k\neq l}}^{l+2K}\mathbf{a}_k s_k + \mathbf{n}_l\right)\left(\sum_{\substack{k=l-2K\\k\neq l}}^{l+2K}\mathbf{a}_k s_k + \mathbf{n}_l\right)^H\right\} = \sum_{\substack{k=l-2K\\k\neq l}}^{l+2K}\mathbf{a}_k\mathbf{a}_k^H\sigma_{\text{s}}^2 + \mathbf{N}_l \tag{36}$$

where $\mathbf{N}_l = \mathbb{E}\left\{\mathbf{n}_l\mathbf{n}_l^H\right\}$ and N_l is the l-th element in the main diagonal of the matrix

$$\mathbf{N}_l = \text{diag}\left[\sigma_{\text{n}}^2 \ \cdots \ \sigma_{\text{n}}^2 \left(\sigma_{\text{n}}^2 + \frac{1}{K}\sum_{m=1}^{K}\frac{|\gamma_{l-K,l}|^2\sigma_{\text{n}}^2}{\left(\tilde{P}_{l-2K+m-1,l-K}\right)^2}\right.\right.$$

$$+\frac{1}{K}\sum_{m=1}^{K}\frac{|\gamma_{l+1,l}|^2\sigma_{\mathrm{n}}^2}{\left(\tilde{P}_{l-K+m,l+1}\right)^2}\Bigg)\left(\sigma_{\mathrm{n}}^2+\frac{1}{K}\sum_{m=1}^{K}\frac{|\gamma_{l-K+1,l}|^2\sigma_{\mathrm{n}}^2}{\left(\tilde{P}_{l-2K+m,l-K+1}\right)^2}+\frac{1}{K}\sum_{m=1}^{K}\frac{|\gamma_{l+2,l}|^2\sigma_{\mathrm{n}}^2}{\left(\tilde{P}_{l+1-K+m,l+2}\right)^2}\right)\cdots\left(\sigma_{\mathrm{n}}^2+\frac{1}{K}\sum_{m=1}^{K}\frac{|\gamma_{l,l}|^2\sigma_{\mathrm{n}}^2}{\left(\tilde{P}_{l-K+m-1,l}\right)^2}\right)\Bigg]^T \in \mathbb{R}^{1\times 2K+2} \tag{37}$$

for TAS1 and

$$\mathbf{N}_l=\mathrm{diag}\Bigg[\sigma_{\mathrm{n}}^2\quad\cdots\quad\sigma_{\mathrm{n}}^2\left(\sigma_{\mathrm{n}}^2+\frac{1}{K}\sum_{k=l-K}^{l+K}|\gamma_{k,l}|^2\sum_{m=1}^{K}\frac{\sigma_{\mathrm{n}}^2}{\left(\tilde{P}_{k-K+m-1,k}\right)^2}\right)\Bigg]^T \in \mathbb{R}^{1\times K+2} \tag{38}$$

for TAS2.

In the case of TAS2 and $K=1$, substituting $\mathbf{R}_{y_l}$ and $\mathbf{R}_{w_l}$ results in (47), as shown at the bottom of the next page, from appendix A. By solving the determinants, (39), as shown at the bottom of this page, is obtained.

Similarly, by computing $\frac{|\mathbf{R}_{\mathbf{y}_l}|}{|\mathbf{R}_{\mathbf{w}_l}|}$ for TAS2 $K>1$, it can be generalized that that $\mathrm{SNR}_l^{\mathrm{TAS2}}$ results in

$$\mathrm{SNR}_l^{\mathrm{TAS2}}=\frac{|\gamma_{l,l}|^2\sigma_{\mathrm{s}}^2}{N_{K+1}}+\frac{\left(\mathbf{h}_{\mathrm{cluster}_1}^{\mathrm{TAS2},K+1}(1)+\mathbf{h}_{\mathrm{cluster}_2}^{\mathrm{TAS2},K+1}(1)\right)^2\sigma_{\mathrm{s}}^2}{N_{K+2}+Y_l^{\mathrm{TAS2}}\sigma_{\mathrm{s}}^2+\sum_{k=l-K}^{l-1}\Upsilon_{k,l}^{\mathrm{TAS2}}} \tag{40}$$

where

$$Y_l^{\mathrm{TAS}n}=\sum_{k=1}^{K}\left(\sum_{m=1}^{K+1}\mathbf{h}_{\mathrm{left}}^{\mathrm{TAS}n,k}(m)\right)^2+\sum_{k=1}^{K}\left(\sum_{m=1}^{K+1}\mathbf{h}_{\mathrm{right}}^{\mathrm{TAS}n,k}(m)\right)^2 \tag{41}$$

and $\Upsilon_{k,l}^{\mathrm{TAS2}}$ is defined in equation (42), as shown at the bottom of this page, where $\mathbf{h}_{\mathrm{cluster}_+}^{\mathrm{TAS}n,k}(m)=\mathbf{h}_{\mathrm{cluster}_1}^{\mathrm{TAS}n,k}(m)+\mathbf{h}_{\mathrm{cluster}_2}^{\mathrm{TAS}n,k}(m)$ and t is the time-slot corresponding to the transmission of BSk. Note that for TAS2, there is only one element in $\mathbf{h}_{\mathrm{text}}^{\mathrm{TAS2},k}(m)$, while for TAS1 there are $K+1$ elements in $\mathbf{h}_{\mathrm{text}}^{\mathrm{TAS1},k}(m)$.

It can be seen that the term $\frac{|\gamma_{l,l}|^2\sigma_s^2}{N_{K+1}}$ in equation (40) corresponds to the SNR received from BSl during the transmission phase. On the other hand the second term corresponds to the contribution of the other BSs in cluster $\mathcal{C}_l$. Specifically, the numerator is the received signal power from all the BSs inside $\mathcal{C}_l$ except BSl and it is divided by the noise power in the last time-slot N_{K+2}, by the received power from the relayed symbols coming from the BSs outside the cluster $Y_l^{\mathrm{TAS2}}\sigma_{\mathrm{s}}^2$, and by $\sum_{k=l-K}^{l-1}\Upsilon_{k,l}^{\mathrm{TAS2}}$, which represents a penalty from the simultaneous transmissions from K BSs inside the cluster during the relaying phase. Note that (40) reduces to (39) for $K=1$.

In the case of TAS1 and $K=1$, substituting $\mathbf{R}_{y_l}$ and $\mathbf{R}_{w_l}$ results in (48), as shown at the bottom of the next page, from appendix B. Solving the determinants results in

$$\mathrm{SNR}_l^{\mathrm{TAS1}}=\frac{|\gamma_{l,l}|^2\sigma_s^2}{N_2}+\frac{\left(\eta_{l-1,l}^{l,l-2}+\eta_{l+1,l}^{l,l}\right)^2\sigma_s^2}{N_3+\left[\left(\eta_{l-1,l}^{l-2,l-2}\right)^2+\left(\eta_{l+1,l}^{l+2,l}\right)^2\right]\sigma_s^2} \tag{43}$$

Computing $\frac{|\mathbf{R}_{\mathbf{y}_l}|}{|\mathbf{R}_{\mathbf{w}_l}|}$ for TAS1 with $K>1$ does not result in a simple closed-form equation. Comparing equations (39) and (43), the difference is in the penalty from the simultaneous transmissions in TAS2, which is not present for TAS1. This makes sense as there are fewer simultaneous transmissions for TAS1 during the relaying phase. Therefore, we propose an expression analogous to (40) as an approximation:

$$\mathrm{SNR}_l^{\mathrm{TAS1}}=\frac{|\gamma_{l,l}|^2\sigma_{\mathrm{s}}^2}{N_{K+1}}+\frac{\left(\sum_{m=1}^{K+1}\mathbf{h}_{\mathrm{cluster}_1}^{\mathrm{TAS1},K+1}(m)+\sum_{m=1}^{K+1}\mathbf{h}_{\mathrm{cluster}_2}^{\mathrm{TAS1},K+1}(m)\right)^2\sigma_{\mathrm{s}}^2}{N_{K+2}+Y_l^{\mathrm{TAS1}}\sigma_{\mathrm{s}}^2}. \tag{44}$$

$$\mathrm{SNR}_l^{\mathrm{TAS2}}=\frac{|\gamma_{l,l}|^2\sigma_s^2}{N_2}+\frac{\left(\eta_{l-1,l}^{l,l-2}+\eta_{l+1,l}^{l,l}\right)^2\sigma_s^2}{N_3+\left[\left(\eta_{l-1,l}^{l-2,l-2}\right)^2+\left(\eta_{l+1,l}^{l+2,l}\right)^2\right]\sigma_s^2+\frac{(\gamma_{l-1,l}\eta_{l,l}^{l+1,l-1}-\gamma_{l+1,l}\eta_{l,l}^{l-1,l-1})^2\sigma_s^4+N_1\left[\left(\eta_{l,l}^{l-1,l-1}\right)^2+\left(\eta_{l,l}^{l+1,l-1}\right)^2\right]\sigma_s^2}{(|\gamma_{l-1,l}|^2+|\gamma_{l+1,l}|^2)\sigma_s^2+N_1}} \tag{39}$$

$$\Upsilon_{k,l}^{\mathrm{TAS2}}=\frac{\left(\gamma_{k,l}\mathbf{h}_{\mathrm{cluster}_+}^{\mathrm{TAS2},k+K+1}(1)-\gamma_{k+K+1,l}\mathbf{h}_{\mathrm{cluster}_+}^{\mathrm{TAS2},k}(1)\right)^2\sigma_{\mathrm{s}}^4+N_t\left[\left(\mathbf{h}_{\mathrm{cluster}_+}^{\mathrm{TAS2},k}(1)\right)^2+\left(\mathbf{h}_{\mathrm{cluster}_+}^{\mathrm{TAS2},k+K+1}(1)\right)^2\right]\sigma_{\mathrm{s}}^2}{\left(|\gamma_{k,l}|^2+|\gamma_{k+K+1,l}|^2\right)\sigma_{\mathrm{s}}^2+N_t} \tag{42}$$

As seen in Section V, this approximation turns out to be quite accurate.

The spectral efficiency per time-slot of Ul for TAS1 and TAS2 is then calculated as

$$S_l^{\mathrm{TAS1}} = \frac{1}{2(K+1)}\mathbb{E}\left\{\log_2\left(1+\mathrm{SNR}_l^{\mathrm{TAS1}}\right)\right\}$$
$$S_l^{\mathrm{TAS2}} = \frac{1}{K+2}\mathbb{E}\left\{\log_2\left(1+\mathrm{SNR}_l^{\mathrm{TAS2}}\right)\right\} \quad (45)$$

The $\frac{1}{2(K+1)}$ and $\frac{1}{K+2}$ scaling factors correspond to the multiplexing gain due to the number of time-slots used for each transmission round. It can be seen that TAS1 and TAS2 can reduce the number of time-slots compared to mSTNC while still achieving diversity from multiple BSs.

The BER of Ul for both schemes using BPSK modulation is given as

$$\mathrm{BER}_l^{\mathrm{TAS}n} = \mathbb{E}\left\{Q\left(\sqrt{2\left(\mathrm{SNR}_l^{\mathrm{TAS}n}\right)}\right)\right\}. \quad (46)$$

V. PERFORMANCE EVALUATION

In this section we compare the performance of TAS1 and TAS2 with the baseline schemes described in Section III. As cellular model, we consider the Wyner model of Fig. 1 with $K = \{1, 2, 4\}$. Our evaluations consider a Rayleigh fading channel model with $\sigma_s^2 = \sigma_n^2 = 1$ and BPSK modulation.

A. EVALUATION WITH EQUAL TRANSMIT POWER AND CHANNEL CONDITIONS

In this section we evaluate the performance of the studied schemes with equal transmit power from all the BSs, i.e. $P_1 = P_2 = P_3 = \cdots = P_l$, and equal average channel gains, i.e. $\mathbb{E}\{|h_{m,l}|^2\} = \mathbb{E}\{|g_{m,n}|^2\} = 1\ \forall m, l, n$.

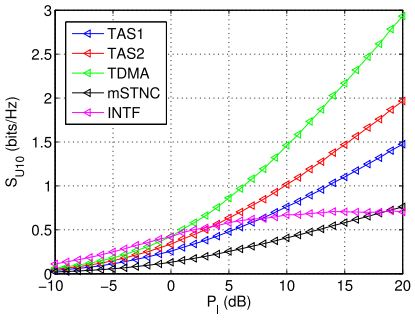

FIGURE 3. Spectral efficiency per time-slot of the different schemes with $K = 1$ and equal transmit power and channel conditions.

The spectral efficiency per time-slot as a function of the transmit power is depicted in Figs. 3, 4, and 5 for $K = \{1, 2, 4\}$, respectively. It can be seen that TDMA has the highest performance followed by TAS2 and TAS1. This is mainly due to the multiplexing gain achieved by reducing the number of time-slots per transmission round. With equal transmit power and equal average channel conditions, the SNR received by Ul from BSl is similar to that received by other BSs inside the cluster, hence TDMA turns out to be the best strategy. However, the difference with respect to TAS2 decreases as K increases. Notice also the large penalty in the spectral efficiency for mSTNC due to the large number of time-slots required to achieve full diversity and the low performance of INTF that floors at 0dB because of the increasing interference.

The BER performance of the different schemes is depicted in Fig. 6. It can be seen that INTF and mSTNC correspond to the upper and lower bounds of the BER, respectively. At this point it is interesting to recall that mSTNC achieves a low BER and full diversity gain at the cost of a large number

$$\frac{|\mathbf{R}_{y_l}|}{|\mathbf{R}_{w_l}|} = \frac{\begin{vmatrix} \left[(\mathbf{b}^2(1))^2 + (\mathbf{b}^4(1))^2\right]\sigma_s^2 + N_1 & 0 & \left[\mathbf{b}^2(1)\mathbf{b}^2(3) + \mathbf{b}^4(1)\mathbf{b}^4(3)\right]\sigma_s^2 \\ 0 & (\mathbf{b}^3(2))^2\sigma_s^2 + N_2 & \mathbf{b}^3(2)\mathbf{b}^3(3)\sigma_s^2 \\ \left[\mathbf{b}^2(1)\mathbf{b}^2(3) + \mathbf{b}^4(1)\mathbf{b}^4(3)\right]\sigma_s^2 & \mathbf{b}^3(2)\mathbf{b}^3(3)\sigma_s^2 & \left[(\mathbf{b}^1(3))^2 + (\mathbf{b}^2(3))^2 + (\mathbf{b}^3(3))^2 + (\mathbf{b}^4(3))^2 + (\mathbf{b}^5(3))^2\right]\sigma_s^2 + N_3 \end{vmatrix}}{\begin{vmatrix} \left((\mathbf{b}^2(1))^2 + (\mathbf{b}^4(1))^2\right)\sigma_s^2 + N_1 & 0 & \left[\mathbf{b}^2(1)\mathbf{b}^2(3) + \mathbf{b}^4(1)\mathbf{b}^4(3)\right]\sigma_s^2 \\ 0 & N_2 & 0 \\ \left[\mathbf{b}^2(1)\mathbf{b}^2(3) + \mathbf{b}^4(1)\mathbf{b}^4(3)\right]\sigma_s^2 & 0 & \left[(\mathbf{b}^1(3))^2 + (\mathbf{b}^2(3))^2 + (\mathbf{b}^4(3))^2 + (\mathbf{b}^5(3))^2\right]\sigma_s^2 + N_3 \end{vmatrix}} \quad (47)$$

$$\frac{|\mathbf{R}_{y_l}|}{|\mathbf{R}_{w_l}|} = \frac{\begin{vmatrix} \left[(\mathbf{c}^2(1))^2 + (\mathbf{c}^4(1))^2\right]\sigma_s^2 + N_1 & 0 & 0 & \left[\mathbf{c}^2(1)\mathbf{c}^2(4) + \mathbf{c}^4(1)\mathbf{c}^4(4)\right]\sigma_s^2 \\ 0 & (\mathbf{c}^3(2))^2\sigma_s^2 + N_2 & \mathbf{c}^3(2)\mathbf{c}^3(3)\sigma_s^2 & 0 \\ 0 & \mathbf{c}^3(2)\mathbf{c}^3(3)\sigma_s^2 & \left[\left(\mathbf{c}^1(3)\right)^2 + (\mathbf{c}^3(3))^2 + (\mathbf{c}^5(3))^2\right]\sigma_s^2 + N_3 & 0 \\ \left[\mathbf{c}^2(1)\mathbf{c}^2(4) + \mathbf{c}^4(1)\mathbf{c}^4(4)\right]\sigma_s^2 & 0 & 0 & \left[(\mathbf{c}^2(4))^2 + (\mathbf{c}^4(4))^2\right]\sigma_s^2 + N_4 \end{vmatrix}}{\begin{vmatrix} \left[(\mathbf{c}^2(1))^2 + (\mathbf{c}^4(1))^2\right]\sigma_s^2 + N_1 & 0 & 0 & \left[\mathbf{c}^2(1)\mathbf{c}^2(4) + \mathbf{c}^4(1)\mathbf{c}^4(4)\right]\sigma_s^2 \\ 0 & N_2 & 0 & 0 \\ 0 & 0 & \left[(\mathbf{c}^1(3))^2 + (\mathbf{c}^5(3))^2\right]\sigma_s^2 + N_3 & 0 \\ \left[\mathbf{c}^2(1)\mathbf{c}^2(4) + \mathbf{c}^4(1)\mathbf{c}^4(4)\right]\sigma_s^2 & 0 & 0 & \left[(\mathbf{c}^2(4))^2 + (\mathbf{c}^4(4))^2\right]\sigma_s^2 + N_4 \end{vmatrix}} \quad (48)$$

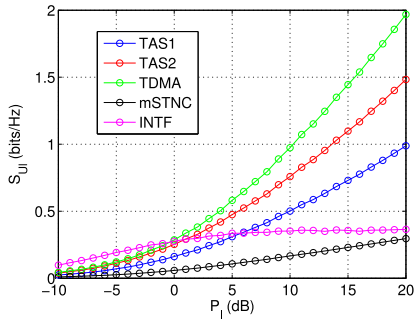

FIGURE 4. Spectral efficiency per time-slot of the different schemes with $K = 2$ and equal transmit power and channel conditions.

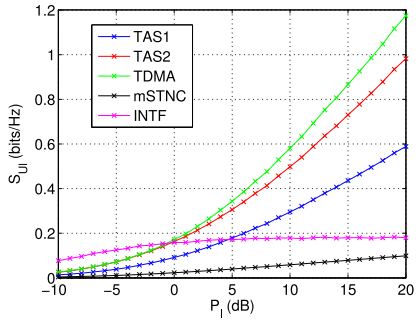

FIGURE 5. Spectral efficiency per time-slot of the different schemes with $K = 4$ and equal transmit power and channel conditions.

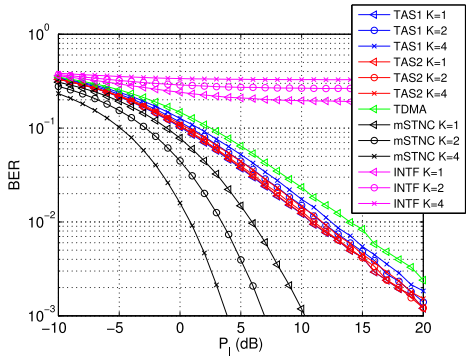

FIGURE 6. BER of the different schemes with equal transmit power and channel conditions.

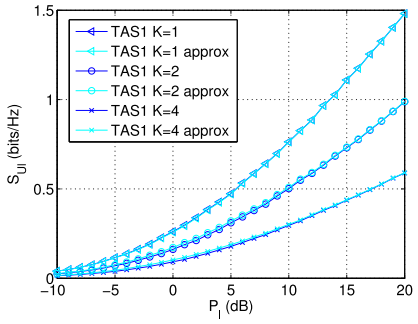

FIGURE 7. Spectral efficiency per time-slot of TAS1.

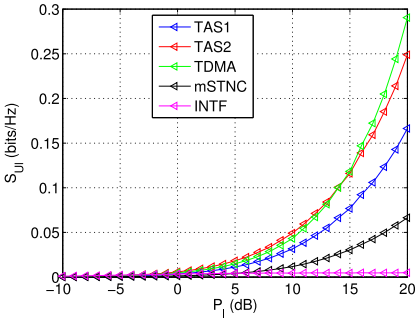

FIGURE 8. Spectral efficiency per time-slot of the different schemes for $K = 2$ with unequal transmit power and equal average channel gains, i.e. $\mathbb{E}\{|h_{m,l}|^2\} = \mathbb{E}\{|g_{m,n}|^2\} = 1\ \forall m, l, n$.

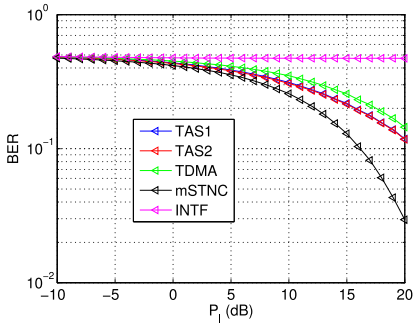

FIGURE 9. BER of the different schemes for $K = 2$ with unequal transmit power and equal average channel gains, i.e. $\mathbb{E}\{|h_{m,l}|^2\} = \mathbb{E}\{|g_{m,n}|^2\} = 1\ \forall m, l, n$.

of time-slots. However, TAS1 and TAS2 achieve a BER lower than INTF and TDMA. Therefore, by taking advantage of the network topology, TAS1 and TAS2 provide a trade-off between multiplexing gain and diversity.

It is worth to note the small difference in BER of TAS1 and TAS2 for different values of K. As K increases, more BSs are able to retransmit a given symbol providing a higher spatial diversity. At the same time, each BS retransmits *more* symbols that interfere with the decoding of the desired symbol. These two opposing effects prevent the BER from decreasing with K.

We also show the spectral efficiency of the approximation for TAS1 compared to its exact value in Fig. 7. It can be seen that the approximation is exact for $K = 1$ and very accurate for $K > 1$. The advantage of this approximation for TAS1 is that it corresponds to a closed-form expression that allows us to analyze and predict the achievable gains for any cluster size and to compare it with other schemes.

B. EVALUATION WITH UNEQUAL TRANSMIT POWER AND CHANNEL CONDITIONS

In this section we evaluate the performance of the studied schemes with unequal transmit power and unequal average channel conditions. For simplicity we only present the case of $K = 2$.

First we analyze the case where BSl has a transmit power 10dB lower than the rest of the BSs, but with equal average channel gains such that $\mathbb{E}\{|h_{m,l}|^2\} = \mathbb{E}\{|g_{m,n}|^2\} = 1\ \forall m, l, n$.

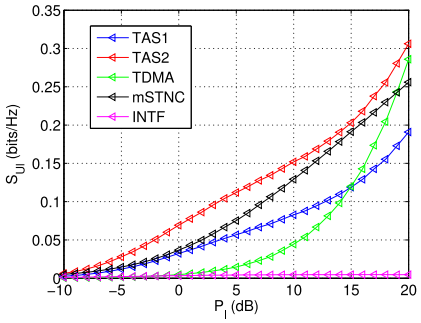

FIGURE 10. Spectral efficiency per time-slot of the different schemes for $K = 2$ with equal transmit power and unequal channel conditions, i.e. $\mathbb{E}\{|h_{l,l}|^2\}$ is 10dB lower than the average channel gain of the rest of the links.

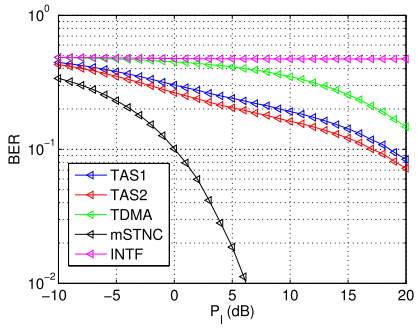

FIGURE 11. BER of the different schemes for $K = 2$ with equal transmit power and unequal channel conditions, i.e. $\mathbb{E}\{|h_{l,l}|^2\}$ is 10dB lower than the average channel gain of the rest of the links.

The spectral efficiency per time-slot and BER in this case is depicted in Figs. 8 and 9, respectively. Then we analyze the case where the average channel gain of Ul, i.e. $\mathbb{E}\{|h_{l,l}|^2\}$, is 10dB lower than the average channel gain of the rest of the links (and equal transmit power from all the BSs). The spectral efficiency per time-slot and BER in this case is depicted in Figs. 10 and 11, respectively. Finally, we analyze the case where the average channel gain of Ul, i.e. $\mathbb{E}\{|h_{l,l}|^2\}$, and the average channel gain between all the BSs, i.e. $\mathbb{E}\{|g_{m,n}|^2\}$ $\forall m, n$, are 10dB lower than the average channel gain of the rest of the links (and equal transmit power from all the BSs). The spectral efficiency per time-slot and BER in this case is depicted in Figs. 12 and 13, respectively.

In the the first case, TAS2 presents a similar spectral efficiency as TDMA followed by TAS1 as seen in Fig. 8. In the second case, the performance difference between TAS2 and TDMA is larger as seen in Fig. 10. This is because, in the first case, the lower transmit power affects the received SNR of Ul, but it also affects the SNR received by the other BSs of the cluster. Hence the gain provided by relaying is limited. In the second case, the lower channel gain only affects Ul and therefore, TAS1 and TAS2 are able to exploit the diversity from the neighboring BSs to provide a higher received SNR to Ul. In terms of BER the differences between mSTNC, TAS1, TAS2, and TDMA increase when comparing unequal transmit power and unequal channel gains as seen in Fig. 9 and Fig. 11.

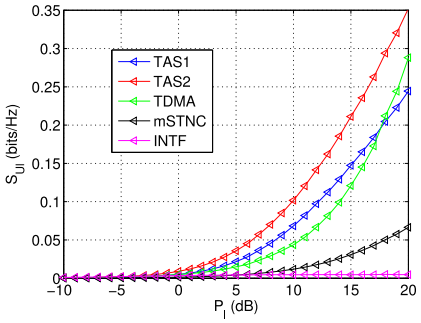

FIGURE 12. Spectral efficiency per time-slot of the different schemes for $K = 2$ with equal transmit power and unequal channel conditions, i.e. $\mathbb{E}\{|h_{l,l}|^2\}$ and $\mathbb{E}\{|g_{m,n}|^2\}$ $\forall m, n$ are 10dB lower than the average channel gain of the rest of the links.

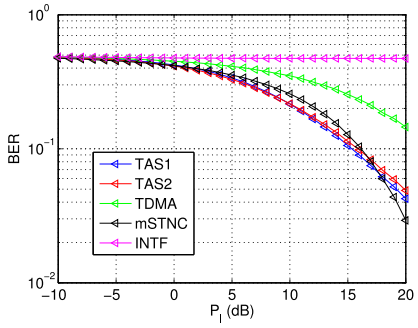

FIGURE 13. BER of the different schemes for $K = 2$ with equal transmit power and unequal channel conditions, i.e. $\mathbb{E}\{|h_{l,l}|^2\}$ and $\mathbb{E}\{|g_{m,n}|^2\}$ $\forall m, n$ are 10dB lower than the average channel gain of the rest of the links.

Finally, in the third case, when the average channel gain of Ul and the average channel gain between BSs are lower than the rest of the links, we can see that mSTNC has the largest performance penalty in spectral efficiency (Fig. 12) and BER (Fig. 13). In this case, TAS2 has the best performance in spectral efficiency and TAS1 has slightly the best performance in BER followed by TAS2.

VI. CONCLUSIONS

In this paper we have proposed two topology-aware STNC schemes that exploit basic knowledge of the network topology, i.e. the knowledge of the subset of BSs that can be overheard by each BS and user, in particular using the Wyner cellular model. This is achieved by allowing simultaneous transmissions from the BSs that do not overhear each other during the transmission phase. In the relaying phase, each BS transmits the information overheard during the transmission phase in two ways. With TAS1, BSs that do not overhear each other transmit simultaneously. With TAS2, all the BSs transmit in one single time-slot. Our results show that TAS1 and TAS2 can improve the spectral efficiency per time-slot and BER with unequal transmit power and unequal channel conditions compared to traditional STNC and other baseline schemes.

APPENDIX A

For TAS2 and $K = 1$, computing $\frac{|\mathbf{R}_{\mathbf{y}_l}|}{|\mathbf{R}_{\mathbf{w}_l}|}$ results in equation (47), where $\mathbf{b}^k(m)$ is the m-th element of the k-th column in matrix $\mathbf{B}$ in (17).

APPENDIX B

For TAS1 and $K = 1$, computing $\frac{|\mathbf{R}_{\mathbf{y}_l}|}{|\mathbf{R}_{\mathbf{w}_l}|}$ results in equation (48), where $\mathbf{c}^k(m)$ is the m-th element of the k-th column in matrix $\mathbf{C}$ in (16).

ACKNOWLEDGMENT

This research work was carried out at the ESAT Laboratory of KU Leuven, in the frame of KU Leuven Research Council PFV/10/002 (OPTEC), FWO project G091213N "Cross-layer optimization with real-time adaptive dynamic spectrum management for fourth generation broadband access networks", and the Belgian Programme on Interuniversity Attraction Poles initiated by the Belgian Federal Science Policy Office "Belgian network on stochastic modeling, analysis, design and optimization of communication systems (BESTCOM)" 2012–2017. The scientific responsibility is assumed by the authors.

REFERENCES

[1] S. Jagannathan, H. Aghajan, and A. Goldsmith, "The effect of time synchronization errors on the performance of cooperative MISO systems," in *Proc. IEEE Global Telecommun. Conf. Workshops (GlobeCom Workshops)*, Nov. 2004, pp. 102–107.

[2] J. Zhang, C. Shen, G. Deng, and Y. Wang, "Timing and frequency synchronization for cooperative relay networks," in *Proc. IEEE Veh. Technol. Conf. (VTC)*, Sep. 2013, pp. 1–5.

[3] H.-Q. Lai and K. J. R. Liu, "Space-time network coding," *IEEE Trans. Signal Process.*, vol. 59, no. 4, pp. 1706–1718, Apr. 2011.

[4] K. Xiong, P. Fan, T. Li, and K. B. Letaief, "Outage probability of space–time network coding over Rayleigh fading channels," *IEEE Trans. Veh. Technol.*, vol. 63, no. 4, pp. 1965–1970, May 2014.

[5] Y. Zhang, K. Xiong, P. Fan, H.-C. Yang, and X. Zhou, "Space-time network coding with multiple AF relays over Nakagami-*m* fading channels," *IEEE Trans. Veh. Technol.*, vol. 66, no. 7, pp. 6026–6036, Jul. 2017.

[6] K. Yang, N. Yang, C. Xing, J. Wu, and Z. Zhang, "Space-time network coding with transmit antenna selection and maximal-ratio combining," *IEEE Trans. Wireless Commun.*, vol. 14, no. 4, pp. 2106–2117, Apr. 2015.

[7] Z. Gao, H.-Q. Lai, and K. J. R. Liu, "Differential space-time network coding for multi-source cooperative communications," *IEEE Trans. Commun.*, vol. 59, no. 11, pp. 3146–3157, Nov. 2011.

[8] K. Xiong, P. Fan, H.-C. Yang, and K. B. Letaief, "Space-time network coding with overhearing relays," *IEEE Trans. Wireless Commun.*, vol. 13, no. 7, pp. 3567–3582, Jul. 2014.

[9] Y. Zhang, K. Xiong, P. Fan, X. Di, and X. Zhou, "Outage performance of space-time network coding with overhearing AF relays," *IEEE Commun. Lett.*, vol. 19, no. 12, pp. 2234–2237, Dec. 2015.

[10] W. Guan and K. J. R. Liu, "Clustering based space-time network coding," in *Proc. IEEE Global Commun. Conf. (GLOBECOM)*, Dec. 2012, pp. 5633–5638.

[11] M. W. Baidas and A. B. MacKenzie, "Many-to-many space-time network coding for amplify-and-forward cooperative networks: Node selection and performance analysis," *EURASIP J. Wireless Commun. Netw.*, vol. 48, Dec. 2014.

[12] C. Geng, N. Naderializadeh, S. Avestimehr, and S. A. Jafar, "On the optimality of treating interference as noise," *IEEE Trans. Inf. Theory*, vol. 61, no. 4, pp. 1753–1767, Apr. 2015.

[13] M. O. Damen and A. R. Hammons, "Delay-tolerant distributed-TAST codes for cooperative diversity," *IEEE Trans. Inf. Theory*, vol. 53, no. 10, pp. 3755–3773, Oct. 2007.

[14] J. Xu, J. Zhang, and J. G. Andrews, "On the accuracy of the wyner model in cellular networks," *IEEE Trans. Wireless Commun.*, vol. 10, no. 9, pp. 3098–3109, Sep. 2011.

[15] M. K. Simon and M. S. Alouini, *Digital Communication Over Fading Channels: A Unified Approach to Performance Analysis*. Hoboken, NJ, USA: Wiley, 2000.

[16] A. Goldsmith, *Wireless Communication*. Cambridge, U.K.: Cambridge Univ. Press, 2005.

[17] T. Cover and J. Thomas, *Elements of Information Theory*. Hoboken, NJ, USA; Wiley, 1991.

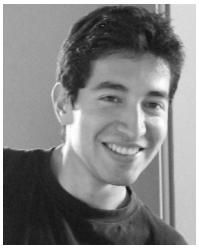

RODOLFO TORREA-DURAN (S'13–M'17) was born in Mexico City, Mexico, in 1981. He received the B.S. in electrical engineering from the Tecnológico de Monterrey Campus Ciudad de Mexico (ITESM-CCM) in 2004 and the master's in information technologies degree (Hons.) from the Universidad Politécnica de Catalunya, Spain, and Université Catholique de Louvain, Louvain-la-Neuve, in 2007. He received the Ph.D. degree from Katholieke Universiteit Leuven in 2017. From 2007 to 2013, he was with the Digital Wireless Group, IMEC, Leuven as a Wireless Research Engineer. His research interests include energy optimization in wireless standards, such as LTE and WLAN and cooperative systems and heterogeneous networks.

MÁXIMO MORALES CÉSPEDES (S'10–M'15) was born in Valdepeñas, Spain, in 1986. He received the B.Sc., M.Sc., and Ph.D. degrees from the Universidad Carlos III de Madrid, Spain, in 2010, 2012, and 2015, respectively, all in electrical engineering, with a specialization in multimedia and communications. From 2015 to 2017, he has been a Post-Doctoral Fellow with the Institute of Information and Communication Technologies, Electronics and Applied Mathematics, Universite Catholique de Louvain. He is currently with the Department of Signal Theory and Communications, Universidad Carlos III de Madrid, Spain. His research interests are interference management, hardware implementations, MIMO techniques, and signal processing applied to wireless communications. In 2012, he was the finalist of the IEEE Region eight Student Paper Contest.

JORGE PLATA-CHAVES (S'09–M'13) was born in Madrid, Spain, in 1984. He received the B.Sc., M.Sc., and Ph.D. degrees from the Universidad Carlos III de Madrid, Spain, in 2007, 2009, and 2012, respectively, all in electrical engineering, with a specialization in multimedia and communications.

From 2007 to 2012, he was with the Department of Signal Theory and Communications, Universidad de Carlos III de Madrid, Spain. From 2012 to 2013, he has been an ER Marie Curie Fellow with the Research Academic Computer Technology Institute, Patras, Greece. He is currently a Post-Doctoral Fellow with the Electrical Engineering Department, KU Leuven. His research interests are in information theory and statistical signal processing with application to interference management in cellular networks and detection, estimation and localization in wireless mobile sensor networks and smart grids.

LUC VANDENDORPE (M'93–SM'99–F'06) was born in Mouscron, Belgium, in 1962. He received the degree (*summa cum laude*) in electrical engineering and the Ph.D. degree from the Université Catholique de Louvain (UCLouvain), Louvain La Neuve, Belgium, in 1985 and 1991, respectively. Since 1985, he has been with UCLouvain, where he first was in the field of bit rate reduction techniques for video coding. In 1992, he was a Visiting Scientist with TUDelft. From 1992 to 1997, he was a Senior Research Associate with the Belgian NSF, UCLouvain, and an invited Assistant Professor. He is currently a Full Professor with the Institute for Information and Communication Technologies, Electronics, and Applied Mathematics, UCLouvain. His research interests include digital communication systems and more precisely resource allocation for OFDM (A)-based multicell systems, MIMO and distributed MIMO, sensor networks, UWB-based positioning, and wireless power transfer. He has been a TPC Member for numerous IEEE conferences (VTC, Globecom, SPAWC, ICC, PIMRC, and WCNC). He was an Elected member of the Signal Processing for Communications Committee from 2000 to 2005, and an Elected Member of the Sensor Array and Multichannel Signal Processing Committee of the Signal Processing Society between 2006 and 2008, and between 2009 and 2011. He was a Co-Technical Chair for the IEEE ICASSP 2006. He was the Chair of the IEEE Benelux joint chapter on communications and vehicular technology between 1999 and 2003, and of the Benelux Section in 2013 and 2014. He served as an Editor for Synchronization and Equalization of the IEEE TRANSACTIONS on COMMUNICATIONS from 2000 to 2002, and as an Associate Editor of the IEEE TRANSACTIONS on WIRELESS COMMUNICATIONS from 2003 to 2005, and the IEEE TRANSACTIONS on SIGNAL PROCESSING from 2004 to 2006.

MARC MOONEN (M'94–SM'06–F'07) is currently a Full Professor with the Electrical Engineering Department, KU Leuven, where he is heading a Research Team involved in the area of numerical algorithms and signal processing for digital communications, wireless communications, DSL, and audio signal processing. He received the 1994 KU Leuven Research Council Award, the 1997 Alcatel Bell (Belgium) Award (with Piet Vandaele), the 2004 Alcatel Bell (Belgium) Award (with Raphael Cendrillon), and was a 1997 Laureate of the Belgium Royal Academy of Science. He received Journal Best Paper Awards from the IEEE TRANSACTIONS on SIGNAL PROCESSING (with Geert Leus and with Daniele Giacobello) and from *Elsevier Signal Processing* (with Simon Doclo).

He was the Chairman of the IEEE Benelux Signal Processing Chapter from 1998 to 2002, a member of the IEEE Signal Processing Society Technical Committee on Signal Processing for Communications, and President of EURASIP from 2007 to 2008 and from 2011 to 2012. He has served as Editor-in-Chief for the EURASIP Journal on Applied Signal Processing from 2003 to 2005, Area Editor for Feature Articles in *IEEE Signal Processing Magazine* from 2012 to 2014, and has been a member of the editorial board of the IEEE TRANSACTIONS on CIRCUITS and SYSTEMS II, *IEEE Signal Processing Magazine*, *Integration-the VLSI Journal*, *EURASIP Journal on Wireless Communications and Networking, and Signal Processing*. He is currently a member of the Editorial Board of *EURASIP Journal on Advances in Signal Processing*.